European Journal of Neuroscience, Vol. 26, pp. 1055–1066, 2007 doi:10.1111/j.1460-9568.2007.05711.x

Distinct movement parameters are represented by different neurons in the motor cortex

Eran Stark,[1] Rotem Drori,[1,2] Itay Asher,[1,2] Yoram Ben-Shaul[3] and Moshe Abeles[1,2,4]
[1]Department of Physiology, Hadassah Medical School, Hebrew University, Jerusalem 91120, Israel
[2]The Interdisciplinary Center for Neural Computation, Hebrew University, Jerusalem, Israel
[3]Department of Neurobiology, Duke University Medical Center, Durham, NC, USA
[4]Gonda Brain Research Center, Bar-Ilan University, Ramat-Gan, Israel

Keywords: extra-cellular recordings, macaque monkey, movement kinematics, temporal correlations

Abstract

Recent studies suggested that a single motor cortical neuron typically encodes multiple movement parameters, but parameters often display strong temporal interdependencies. To address this issue, we recorded single-unit activity while macaque monkeys made continuous movements and employed an analysis that explicitly considered temporal correlations between several kinematic parameters; hand position, velocity, and acceleration. We found that while the activity of almost all motor cortical neurons was modulated during movement, most neurons were related only to a single dominant parameter. The activity of different neurons covaried with different parameters with similar strength, but neurons related to velocity were far more common than neurons related to any other parameter. These results were obtained for neurons recorded in the primary motor (M1) and dorsal premotor (PMd) cortices. Although neural activity tended to precede movement and PMd activity tended to precede M1 activity, time lags were widely dispersed. Shoulder and elbow muscles had the same properties as neurons, but their activity strictly preceded movement. These results demonstrate single neuron specificity and heterogeneity within a population of neurons with respect to movement parameters and time lags. Our results suggest that distinct subsets of motor cortical neurons are involved in computations related to distinct movement parameters.

Introduction

Understanding how the brain plans and controls motion depends to a great extent on understanding how movement parameters are encoded in the activity of neurons in the motor cortex. The activity of motor cortical neurons has been related to almost every tested parameter (Thach, 1978), including isometric force (Evarts, 1968; Georgopoulos *et al*., 1992; Sergio *et al*., 2005), muscle activity (Fetz & Cheney, 1980; Crutcher & Alexander, 1990; Park *et al*., 2004), joint torques (Riehle & Requin, 1995; Scott & Kalaska, 1997), joint angles (Aflalo & Graziano, 2006), changes in joint angles (Reina *et al*., 2001), and even the serial order of movements (Carpenter *et al*., 1999).

Focusing on movement parameters measured in coordinates extrinsic to the animal, the work of Georgopoulos and colleagues (Georgopoulos *et al*., 1982, 1986) demonstrated that the direction of arm movement is prominently represented in the activity of arm-related motor cortical neurons. Subsequent studies extended these findings by showing that arm posture (Kettner *et al*., 1988; Caminiti *et al*., 1990), hand speed (Moran & Schwartz, 1999), and acceleration (Flament & Hore, 1988) modify the discharge of motor cortical neurons as well. Moreover, studies that assessed multiple parameters found that single neurons in the motor cortex are related to multiple movement parameters (Humphrey *et al*., 1970; Kurata, 1993; Ashe & Georgopoulos, 1994; Fu *et al*., 1995; Messier & Kalaska, 2000; Johnson *et al*., 2001; Paninski *et al*., 2004).

Correspondence: Eran Stark, as above.
E-mail: eran.stark@ekmd.huji.ac.il

Received 18 December 2006, revised 14 May 2007, accepted 18 June 2007

Two main issues complicate the study of relations between movement parameters and neural activity. First, movement parameters and their values are often sampled sparsely. For instance, in a centre-out paradigm (Georgopoulos *et al*., 1982), the required movement directions usually assume eight different values. Even when using continuous curved movements (Schwartz, 1992, 1994; Moran & Schwartz, 1999; Schwartz *et al*., 2004), there is typically a limited repertoire of stereotypically repeating movements, leading to difficulties in differentiation among parameters. Second, in most experimental designs the tested parameters are interdependent. Dependencies between parameters are observed between extrinsic and intrinsic coordinate frames (Mussa-Ivaldi, 1988; Todorov, 2000; Reina *et al*., 2001) as well as within a coordinate frame. Kinematic movement parameters (position and its time derivatives) measured in extrinsic coordinates are highly correlated with one another. For instance, during movement in a centre-out task, end-point position invariably determines velocity direction, and the velocity and acceleration vectors have colinear directions. Moreover, both simultaneous and delayed correlations may result in ambiguous interpretation of neural activity.

Mitigation of the abovementioned effects can be achieved by employing experimental paradigms that sample the movement parameter space more broadly than the abovementioned studies (for instance, Paninski *et al*., 2004; Aflalo & Graziano, 2006; Jackson *et al*., 2006) and statistical methods that take into account temporal correlations between parameters (as in Stark *et al*., 2006). Here, we combine these ideas. We limit our study of movement parameters to hand kinematics (position, velocity and acceleration) and demonstrate that most single motor cortical neurons are each related to a single predominant movement parameter.

Materials and methods

Animals and behavioural tasks

Two monkeys (female *Macaca fascicularis*, U and F, 3 and 3.5 kg) were used in this study. Animal handling procedures were in accordance with the NIH Guide for the Care & Use of Laboratory Animals (1996), complied with Israeli law, and were approved by the Ethics Committee of the Hebrew University. Monkeys were trained to sit in a primate chair and to perform continuous curved movements with their preferred hand (U, right; F, left) by operating a two-joint low-friction planar manipulandum. The nonpreferred hand was restrained. A horizontal opaque screen, mounted at chest level, blocked the view of manipulandum and hand. A circular cursor indicating hand end-point was projected on the screen (diameter 0.4 cm). Two tasks were employed.

In the scribbling task (Fig. 1A) the monkey saw only the cursor. When the manipulandum end-point, moved by the monkey, was placed inside an invisible hexagon (diagonal of 3.5 cm) a trial was considered successful and the monkey was rewarded by a drop of juice. Immediately, another hexagon was randomly selected and the process repeated (a total of 19 hexagons were tiled symmetrically). The monkey performing this task (U) completed 689 scribbles per session (median; range 499–1076; 18 sessions), each 1.3-s long (median; 95% range 0.1–5.8 s).

In the tracing task (Fig. 1B) the monkey traced given paths at its own pace. During each session 40 different paths were used, each generated by fitting a cubic spline to ten randomly chosen points in a plane (10 × 10 cm). Each path consisted of 90 points (median; range 64–125; centres 0.4 cm apart). At the beginning of a trial, one path was randomly selected and its origin was shown as a green circle. After the monkey placed the cursor inside the origin for a period of 750–1000 ms, the entire path was shown; path points were shown as partially overlapping grey circles (diameter of 0.55). The first eight circles were coloured green. As the monkey moved the cursor into the first green circle, the circle changed colour to grey and the subsequent grey circle in the path turned green, a process repeated until the entire path was traced. A trial was considered successful and the monkey was rewarded if the entire path was traced without pausing for more than 800 ms between successive circles; otherwise, the trial was aborted. The monkey performing this task (F) completed 334 tracing trials per session (median; range 218–487; 22 sessions), each 3.4-s long (median; 95% range 2–5.9 s).

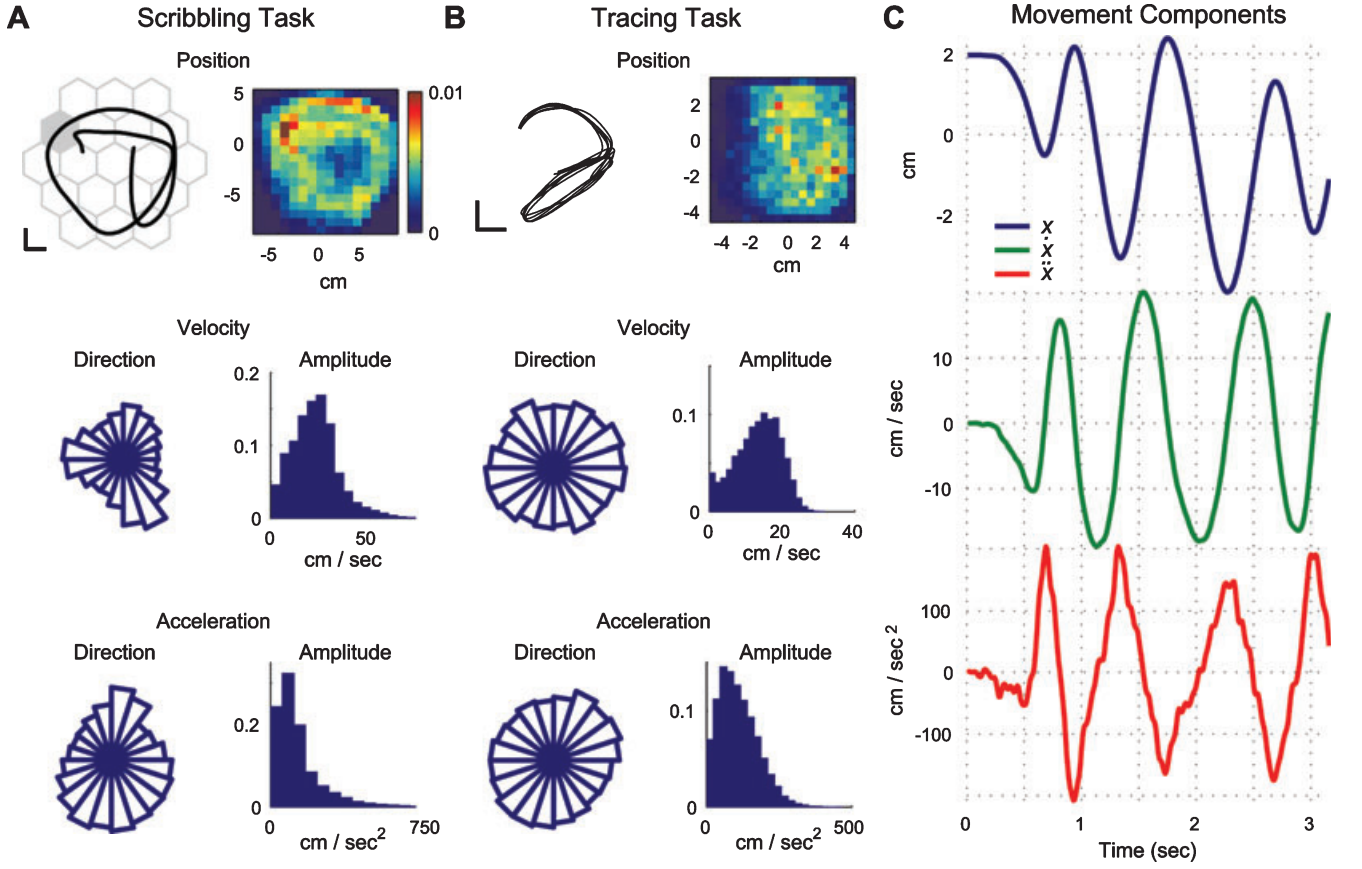

FIG. 1. Movement tasks and distributions of movement parameters. (A) Scribbling task. The top left panel shows a scribble made by a monkey. During scribbling, the monkey moved a two-joint manipulandum in the horizontal plane. Once an invisible target illustrated here by the grey hexagon was entered, the monkey was rewarded, another target was randomly selected, and the process was repeated. Calibration bars, 2 cm. Other panels show distributions of movement parameters during 194 scribbling paths made during the same scribbling session as in the top left panel (mean and SD of trial duration 2.4 ± 1.5 s). In the 2D histogram, the fraction of time spent in each position is presented on a scale from 0 to 0.01 (see calibration bar). In the rose diagrams, the area of each of the 20 sectors is equivalent to the fraction of time spent moving or accelerating in the corresponding direction. (B) Tracing task. The top left panel shows five repetitions of one path drawn by a monkey during one tracing session. During each session, 40 different paths were used. Paths spanned the entire working plane and were traced in a pseudo-random order. The monkey traced each path at its own pace. Other panels show distributions of movement parameters during tracing of 141 paths during the same recording session (average trial duration 3.1 ± 0.9 s). All conventions are the same as in (A). (C) Illustration of temporal relations between horizontal position (x), horizontal component of the velocity vector ($\dot{x}$), and horizontal component of the acceleration vector ($\ddot{x}$). Parameters are plotted for a single tracing trial. In the example, a peak in the position curve is preceded by a peak in velocity by ∼200 ms, and a peak in velocity is preceded by a peak in acceleration by another ∼200 ms. Thus, while movement components have low correlations at zero-lag, delayed correlations are much higher. See Results for more details.

Surgical procedures

Following training, a localizing MRI scan (Biospec Bruker 4.7 T animal system, fast spin echo sequence; effective echo time, 80 ms; repetition time, 2.5 s; 0.5 × 0.5 × 2 mm resolution) was performed. A head-holding apparatus and a plastic recording chamber (27 × 27 mm) were then cemented to the skull using dental acrylic under general anesthesia [halothane anesthesia, induced by medetomidine hydrochloride (Domitor, 0.1 mg/kg) and ketamine (3 mg/kg)]. Analgesia [pentazocine (Talwin) and carprofen (Rymadil)] and antibiotics (ceftriaxone) were administered peri-operatively. The dura mater was left intact.

After completion of experiments, monkeys were deeply anesthetized (ketamine-induced pentobarbital anesthesia, 30 mg/kg) and killed by an overdose of pentobarbital. During this procedure, pins were inserted in defined chamber locations to allow reconstruction of penetration sites relative to cortical landmarks. Then monkeys were perfused transcardially with 0.9% saline followed by 4% formaldehyde in a 0.1 M phosphate buffer. In addition, 50 μm coronal sections were prepared from the right hemisphere of monkey F.

Recording procedures and database

During each recording session up to eight glass-coated tungsten microelectrodes (impedance 0.2–1.5 MΩ at 1 kHz) confined to a guide tube (internal diameter 1.5 mm) were inserted into arm-related regions of the primary motor cortex (M1) or dorsal premotor cortex (PMd) contra-lateral to the preferred hand using a computer-controlled microdrive (EPS, Alpha-Omega Engineering, Nazareth, Israel). Arm relations were assessed by passive limb manipulations and by intracortical microstimulation (ICMS; 150 ms trains of 0.2 ms biphasic pulses at 300 Hz). The boundary between M1 and PMd was estimated on the basis of sulcal landmarks obtained during MRI scans and ICMS thresholds (thresholds for penetrations in M1 were ≤ 40 μA and those in PMd were ≤ 70 μA), and verified by histology (regions where the density of large pyramidal cells changed; Weinrich & Wise, 1982). The output signal of each electrode was amplified (10 K), band-pass filtered (0.3–6 kHz, MCP+, Alpha-Omega Eng), and fed to template matching devices (MSD, Alpha-Omega Eng) to isolate the activity of 1–3 units per electrode. Spikes and behavioural events were sampled at 1 kHz and logged on a custom data-acquisition system. Firing rate profiles were obtained by convolving spike trains with a Gaussian kernel (SD of 50 ms).

Muscle activity was recorded in separate sessions (monkey F) by inserting wire pairs into shoulder (acromion deltoid, pectoralis major, trapezoid) and elbow (biceps brachii, triceps brachii) muscles; each muscle was recorded during 3–4 separate sessions. The differential signals from the wire pairs were amplified (30 K), band-pass filtered (30–3000 Hz), and sampled at 25 kHz (Alpha-Map 5.4, Alpha-Omega Eng). Root mean square values of EMG were computed by raising records to the second power, applying a low-pass filter (100 Hz), and taking the square root. These traces were then processed exactly like the spike trains.

Hand position was sampled at 100 Hz and low-pass filtered (8 Hz). Velocity and acceleration were computed by taking the corresponding derivatives. Position and its time derivatives were expressed in units of cm and s.

All units considered for analysis were (i) well-isolated, as determined by spike waveforms and by interspike interval histograms, and (ii) recorded during a subset of consecutive trials in which activity was first-order stationary. Stationarity was verified quantitatively by computing the mean firing rate for each trial and plotting it against chronological trial number; units that exhibited a significant linear rate trend (quantified by the correlation-coefficient and tested by trial shuffling; 1000 shuffles, $P < 0.05$; Paninski *et al*., 2004) were not considered. The total duration of all considered movement periods was at least 2.5 min. For scribbling movements, the first 200 ms following a reward were excluded. For tracing movements, the considered movement periods started once the monkey began to follow the path and ended once the end of the path was arrived at, before reward was delivered.

Movement model

The firing rate of a unit was modelled as a linear function of movement,

$$F(t) = c + \sum_{i=0}^{2} a_i f(x^{(i)}(t+\tau_i), y^{(i)}(t+\tau_i)). \quad (1)$$

In Eqn (1), the superscript *(i)* indicates the i^{th} derivative of position with respect to time, and τ_i indicates that the i^{th} derivative is lagged (delayed by) τ time samples relative to the firing rate. The value of τ can be positive or negative; positive values correspond to neural activity leading movement. Thus, the firing rate F at time t is a function of the position (x, y) at time $t + \tau_{\text{pos}}$, of the velocity vector at time $t + \tau_{\text{vel}}$, and of the acceleration vector at time $t + \tau_{\text{acc}}$. Individual components were modelled using cosine functions. Specifically, the position component was modelled as a function of the Euclidian distance from an unknown preferred position,

$$f(x,y) = b_x \cos\frac{2\pi}{K_{\text{pos}}}(x - x_0) + b_y \cos\frac{2\pi}{K_{\text{pos}}}(y - y_0). \quad (2)$$

The function peaks at (x_0, y_0) and troughs K_{pos} cm away in both the horizontal and vertical directions. Although results were not sensitive to the precise value of K_{pos}, we employed a constant $K_{\text{pos}} = 10$ cm/rad, which, given workspace sizes, resulted in symmetric uni-modal surfaces. The cosine model was employed rather than a planar model (Kettner *et al*., 1988; Paninski *et al*., 2004) because the discharge of many units appeared to be higher in specific parts of the workspace without an apparent monotonous gradient. However, findings reported below were also obtained when a planar model was employed (see Discussion). The velocity component was modelled as the angular distance from an unknown preferred direction,

$$f(\dot{x},\dot{y}) = \|\vec{v}\|\left(b_{\text{vel}} + \cos\frac{2\pi}{K_{\text{vel}}}(\theta_{\text{vel}} - \theta_0)\right). \quad (3)$$

In Eqn (3), $\dot{x}$ and $\dot{y}$ are the horizontal and vertical components of the velocity vector, $\|\vec{v}\|$ is its magnitude (speed, $\sqrt{\dot{x}^2 + \dot{y}^2}$), and θ_{vel} is its direction $(\tan^{-1}\dot{y}/\dot{x})$.We employed $K_{\text{vel}} = 2\pi$, resulting in a symmetric uni-modal curve with a baseline b_{vel} and a preferred direction at θ_0, scaled by speed (Moran & Schwartz, 1999). A similar expression was used to model the acceleration component.

Multiple regression and statistical significance

By combining Eqn (1–3), Eqn (1) can be rewritten as

$$\begin{aligned} F(t) = {} & b_0 + b_1 \cos kx(t+\tau_{\text{pos}}) + b_2 \sin kx(t+\tau_{\text{pos}}) \\ & + b_3 \cos ky(t+\tau_{\text{pos}}) + b_4 \sin ky(t+\tau_{\text{pos}}) \\ & + b_5\|\vec{v}(t+\tau_{\text{vel}})\| + b_6\dot{x}(t+\tau_{\text{vel}}) + b_7\dot{y}(t+\tau_{\text{vel}}) \\ & + b_8\|\vec{a}(t+\tau_{\text{acc}})\| + b_9\ddot{x}(t+\tau_{\text{acc}}) + b_{10}\ddot{y}(t+\tau_{\text{acc}}) \end{aligned} \quad (4)$$

with $k = 2\pi/10$. Previous studies have suggested that time lags range from −300 to 300 ms (Ashe & Georgopoulos, 1994; Moran &

Schwartz, 1999; Schwartz *et al.*, 2004). We examined the same range with 10 ms resolution for each of the three time lags. For a given combination of lags (τ_{pos}, τ_{vel}, τ_{acc}), the appropriate movement data were lagged relative to the neural data for each trial separately and then data from different trials were combined (Ashe & Georgopoulos, 1994). Subsequently, regression coefficients (b_i) and the total R^2 were estimated using least-squares. Regression coefficients were expressed as standardized coefficients ($\beta_i = b_i \cdot \sigma_i/\sigma_F$, where σ_i is the SD of the i^{th} parameter, $i = 1..10$, and σ_F is the SD of the firing rate F). The R^2 is the fraction of the firing rate variance associated with the movement parameters included in the analysis. In this study, the R^2 is therefore a function of three time lags, and can be visualized as a three-dimensional cube (e.g. Fig. 2A) in which each axis measures the time lag between neural activity and a different movement parameter; position (horizontal), velocity (vertical), and acceleration (depth).

Statistical significance of the R^2 at a given combination of time lags was assessed using two methods. The first method was a parametric F-test, which yielded extremely low P-values, typically lower than 10^{-10}. The F-test assumes, among other assumptions, that residuals are uncorrelated, distributed normally, and that their variance does not depend on the variance of the firing rate (Draper & Smith, 1981). As firing rate is nonnegative, these assumptions were not always met. We therefore employed a second method that did not rely on the above assumptions. By randomly shuffling (permuting) firing rate profiles between trials, correlations between firing rate and movement parameters were abolished, without altering correlations among movement parameters, their auto-correlations, or the firing rate auto-correlations. Because trials were of different lengths, for the purpose of this test only we chose an arbitrary minimal trial duration of 2 s and discarded shorter trials; from longer trials we employed only the central part. For each set of shuffled trials, the R^2 was re-computed. Shuffling was repeated 10 000 times. The unusually high number of shuffles was chosen to account for the multiple comparisons that stem from the many combinations of time lags. If all shuffles yielded R^2s smaller than the value computed for the trimmed – but nonshuffled – trials, the unit was considered movement-related. The uncorrected P-value is then smaller than 0.0001, corresponding to a conservative estimate of a corrected P-value smaller than 0.01 (for a cube spanning

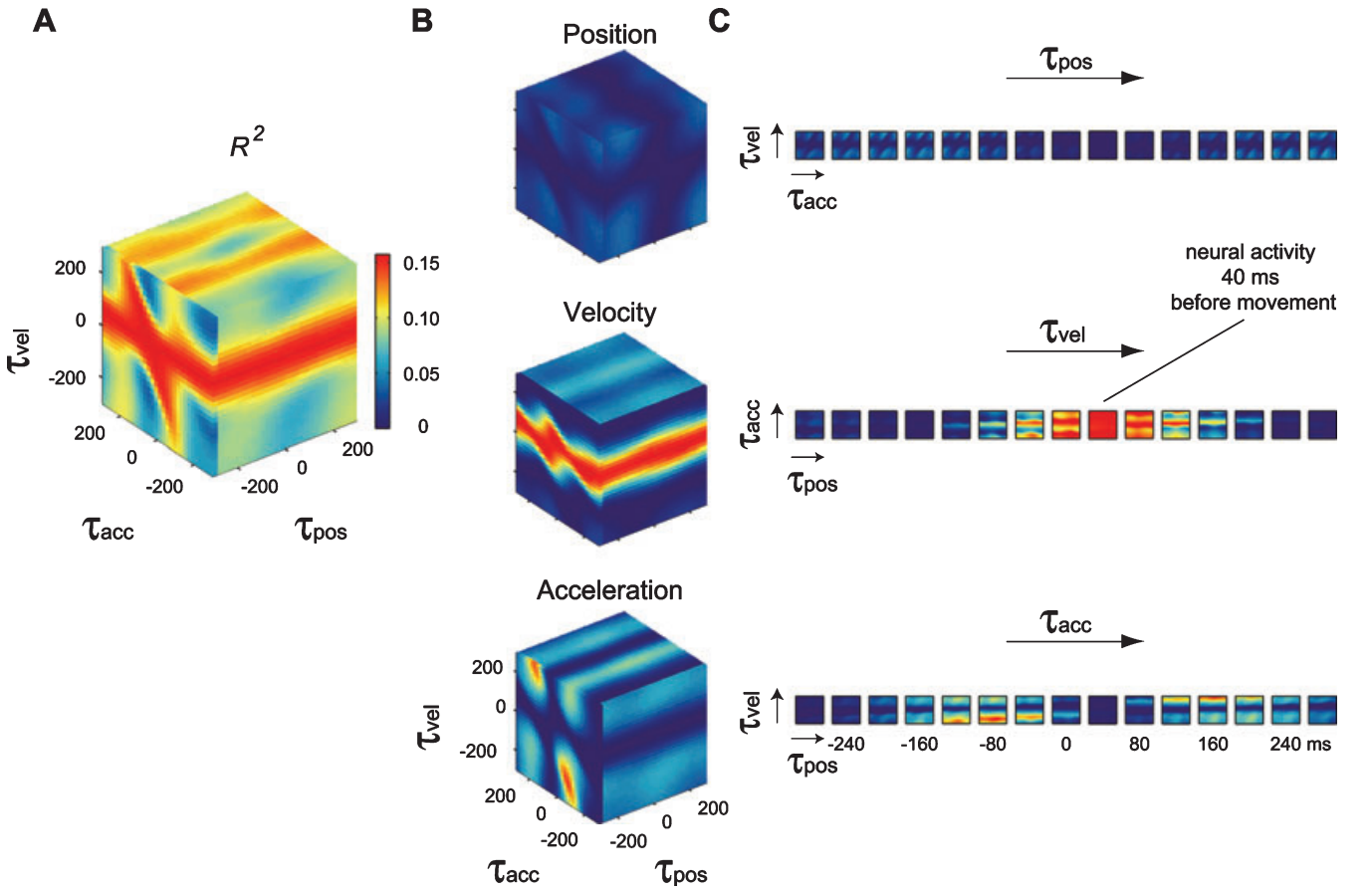

FIG. 2. Illustration of analysis method at multiple time lags. We simulated activity of a putative neuron with a cosine relation to velocity direction; $F(t) = 10 + 6cos\theta_{vel}(t + 50)$. $F(t)$ is the firing rate at time t and θ_{vel} $(t + 50)$ is the direction of the velocity vector 50 ms later. θ_{vel} was derived from real movements. See Materials and methods for details. (A) R^2 cube. Each axis of the cube measures the time lag between neural activity and a different movement parameter; position (horizontal), velocity (vertical), and acceleration (depth). Positive lags correspond to neural activity coming before movement. The scale (see calibration bar) indicates the fraction of firing rate variance associated with the movement parameters, R^2, examined at each combination of time lags. The three faces show the three marginal means, at each dimension. The stripes with highest R^2 values on the velocity-acceleration face (left) and on the velocity-position face (right) suggest a relation with velocity at a constant time lag. (B) Contribution cubes. From top to bottom; contribution of position (taking into account velocity and acceleration), velocity (taking into account position and acceleration), and acceleration (taking into account position and velocity) to the movement-related firing rate variance. There are stripes of relatively high contribution on the velocity cube and not on any other cube. Axes and R^2 scale are the same as in (A). (C) Slicing through each of the cubes at a different orientation, at a given time lag for each parameter, a plane of high contribution is evident in the velocity cube (middle row). The contribution values in this plane are all higher than half the maximal R^2 (0.16 for the putative neuron). There are no planes or any other dominant features in other cubes. For presentation purposes, slices are shown at 40-ms intervals. Examined at a higher temporal resolution, it becomes clear that the correlation with velocity peaks 50 ms before movement (see Materials and methods). Color scale is the same as in A.

600^3 ms estimated for spike trains smoothed by a Gaussian kernel with SD of 50 ms there are less than 100 independent measurements). Although results were not influenced by the choice of method, we report statistics based on the permutation test.

The movement model (Eqn 4) does not account for possible serial correlations in the firing rate, which may arise from auto-correlations within the original spike trains. We thus considered an extended firing rate model; the same as in Eqn (4), with an additive auto-regressive term, $b_{11}F(t - \tau_{AR})$. The negative sign of τ_{AR} indicates that $F(t)$, the firing rate at time t, may depend on the firing rate observed τ_{AR} ms earlier. We considered a 'first-order' auto-regressive model with a fixed $\tau_{AR} = 150$ ms, chosen according to the SD of the Gaussian kernel employed for smoothing (50 ms, which induced auto-correlations in firing rates for time lags up to 150 ms). Thus, correlations persisting at or beyond this lag are of potentially neural origin. The statistical significance of the extended model was tested using the permutation test described above, with a firing rate profile from a randomly selected trial substituting the auto-regressive term. The extended model produced residuals that were uncorrelated at time lags beyond 150 ms but no qualitative changes in the main results of the analysis (see Results).

Estimation of parameters and time lags

To measure the influence of each parameter on firing rate variance we employed the measure of contribution (Scherrer, 1984), estimated at multiple time lags,

$$C_i(\tau_{\text{pos}}, \tau_{\text{vel}}, \tau_{\text{acc}}) = \beta_{\text{i}}(\tau_{\text{pos}}, \tau_{\text{vel}}, \tau_{\text{acc}}) \cdot \rho_i(\tau_i), \quad (5)$$

where β_{i} is the standardized regression coefficient corresponding to the i^{th} parameter ($i = 1..10$), at time lag combination (τ_{pos}, τ_{vel}, τ_{acc}), and $\rho_{\text{i}}(\tau_{\text{i}})$ is the pair-wise (Pearson) correlation-coefficient between firing rate and parameter i, at time lag τ_i. For instance, speed contributions are estimated by $\beta_5(\tau_{\text{pos}},\tau_{\text{vel}},\tau_{\text{acc}}) \cdot \rho_5(\tau_{\text{vel}})$. For each combination of time lags, the sum of all contributions equals the R^2. Thus, the contribution of a specific parameter can be interpreted as a fraction of the total R^2, namely the portion of movement-related firing rate variance associated with that parameter, taking into account all other parameters, at a given combination of time lags. Other often-used measures of importance including P-values, partial R^2s, standardized regression coefficients (βs), or β^2s cannot be interpreted in that manner. The contributions of different parameters of the same time-derivative (position, velocity, or acceleration) were combined, yielding C_{pos}, C_{vel} and C_{acc} (Fig. 2B). The same permutation test used for determining significance of the R^2 was used for testing the significance of C_{pos}, C_{vel}, and C_{acc}.

After determining that firing rate was related to movement by testing the significance of the model (Eqn 4) we determined which movement parameters contributed to the firing rate variance and at what time lags. For artificial neural activity related to velocity, there is a plane of high values in the velocity cube, at a constant τ_{vel} for all τ_{pos}s and all τ_{acc}s (Fig. 2B and C). We therefore looked for parameters that were related to firing rate at a constant time lag manifesting as a plane slicing through the relevant contribution cube, operationally defining a dominant relation to a movement parameter at a given lag as a cube's plane at that lag in which at least half of the time lag combinations each contributes at least half of the maximal R^2. Thus, holding constant the time lag of one parameter, we look – in the cube corresponding to that parameter – for a temporally contiguous ('connected') region of values above $\max(R^2)/2$ corresponding to the time lags of the two other parameters. If most time lag combinations are high and contiguous, a plane is detected. Continuity was required to prevent spurious detections (e.g. of high valued 'zebra stripes') and was determined using the BWLABELN function of the MATLAB image processing toolbox. The above definition allows zero, one, or more parameters to be dominant at the same time lag relative to the firing rate (cf. Fig. 3D). In Fig. 4 we show that the main results are not sensitive to the specifics of this definition.

To make sure that results did not depend on the detection of planes, we also focused on the combination of time lags that yielded the maximal R^2 and calculated the contribution of each parameter at that combination. A dominant parameter was then defined as a parameter that contributed more than half of the movement-related variance at that combination of lags. The same process was repeated for time lag combinations with R^2s close to ($1/\sqrt{2}$ or 90% of) the maximal R^2 with no notable differences.

To determine whether there was an excess of units related to a single dominant parameter, we computed the fractions of units that were related to each parameter. Then, assuming parameters are allocated to units randomly (i.e. with uniform probability), the probability to observe a unit related to exactly one parameter was computed. This probability was then used to estimate the Binomial probability to find the observed or higher number of units related to exactly one parameter.

Simulations and sensitivity analyses

The entire procedure detailed above was tested using simulations. Using real movements from each of the tasks, we first generated noiseless firing rate profiles for each trial according to various models and time lags (as in Stark *et al*., 2006, with the addition of position dependencies and combined dependencies on two and three parameters). Realization of noisy firing rate profiles was carried out by treating the noiseless rate profiles as time-varying Poisson processes and generating spike trains by deciding at every millisecond whether a spike was or was not fired. The artificial trains were then processed exactly like the spike trains recorded in experiments. In all realizations, the firing rate mean and variance were as in real neurons (median mean firing rate 5.2 spike/s, range 1.1–39; median SD of firing rate 6.8 spikes/s, range 2.9–22; 218 units). For artificial neurons with R^2 above 0.02, the correct identity and number of encoded movement parameters was detected in >95% of the cases, with very few misses (false positive rate <5%, false negative rate <1%). Determination of time lags was unbiased, with errors <20 ms.

Results

Explicit consideration of temporal correlations during continuous movements enables the separation of the contributions of movement parameters to neural activity

During scribbling movements (Fig. 1A) the monkey was free to move the manipulandum as it willed. In contrast, during tracing movements (Fig. 1B) the monkey was required to follow predetermined paths. Although some deviation was allowed (Materials and methods), paths were closely followed, with an R^2 of 0.95 (median; 95% range of 7355 trials during 22 sessions, 0.92–0.97; for each trial, R^2s between instructed and actual paths were computed separately for horizontal and vertical coordinates and then averaged). The common feature of both tasks was that a plethora of continuous curved movements were made, so that movement parameters were sampled broadly (Fig. 1A and B). This opened up the possibility for differentiation between the kinematic parameters analysed here; end-point position, the velocity vector, and the acceleration vector. Moreover, zero-lag correlations

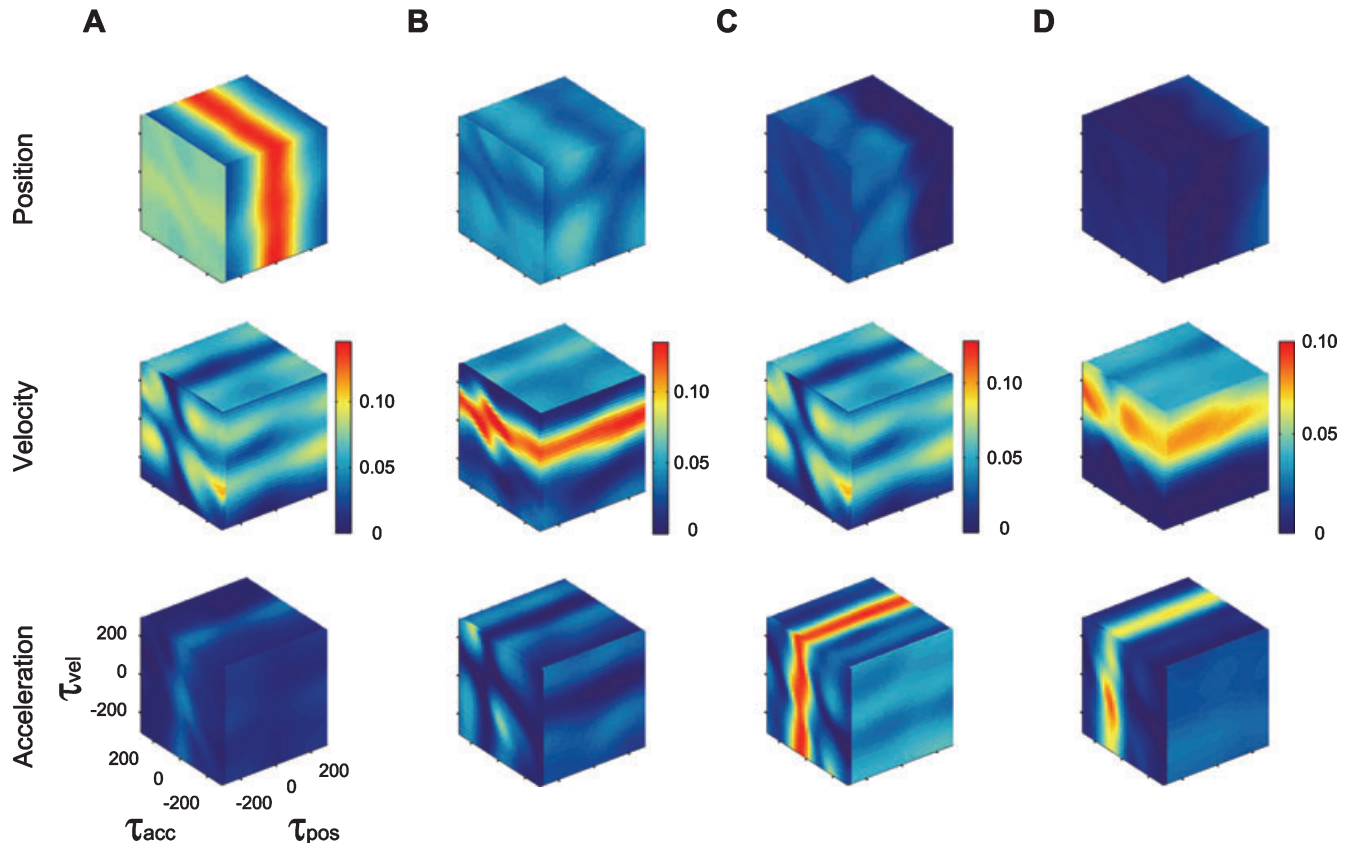

FIG. 3. Correlations between motor cortical neurons and movement parameters. (A) The neural activity is related predominantly to position, peaking at a time lag of 10 ms, irrespective of the delay with either velocity or acceleration. The maximal R^2 for this unit is 0.18 (not shown). The calibration scale is the same for the three contribution cubes. Conventions are the same as in Fig. 2B. Axis labels are detailed in the bottom cube and indicated by small ticks in all other cubes. (B) Neural activity related mainly to velocity. Time lag is 80 ms, R^2 is 0.17. (C) Neural activity related mainly to acceleration. Time lag is 40 ms, R^2 is 0.17. (D) Neural activity related to velocity and acceleration. Time lag is 140 ms for velocity and 80 ms for acceleration. The maximal R^2 is 0.14.

between parameters were substantially reduced in these tasks; mean correlation-coefficients between horizontal components of position (x), velocity ($\dot{x}$), and acceleration ($\ddot{x}$) and their SDs were: 0 ± 0.02 $(x, \dot{x})$ and 0.02 ± 0.02 $(\dot{x}, \ddot{x})$ in the scribbling task (correlation-coefficients were computed separately for every trial and then averaged across all trials in each of 18 sessions), and 0 ± 0.003 $(x, \dot{x})$ and 0.03 ± 0.002 $(\dot{x}, \ddot{x})$ in the tracing task (22 sessions). However, strong correlations typically persisted at delays of approximately 200 ms [Fig. 1C; peak correlation-coefficients during scribbling: 0.18 ± 0.08 at 84 ± 380 ms $(x, \dot{x})$ and 0.54 ± 0.05 at 236 ± 26 ms $(\dot{x}, \ddot{x})$; and during tracing: 0.33 ± 0.02 at 214 ± 11 ms $(x, \dot{x})$ and 0.74 ± 0.01 at 152 ± 7 ms $(\dot{x}, \ddot{x})$]. Therefore, if the activity of a neuron is correlated with the velocity observed 50 ms later, it will also be correlated with the acceleration observed approximately 150 ms earlier. These correlations make it difficult to determine whether the neural activity is related to one parameter, to another, or to both.

However, as movement parameters were not perfectly correlated with one another, the individual contributions of different parameters to the firing rate variance can be isolated by explicitly considering temporal correlations between parameters. For purposes of demonstration, we simulated firing rates based on continuous movements and a model of tuning to a single parameter, velocity direction, $F(t) = 10 + 6cos\theta_{vel}(t + 50)$ (Georgopoulos *et al.*, 1982; baseline and gain parameters were chosen according to Schwartz *et al.*, 1988; see Materials and methods for simulation details). In the latter model, neural activity precedes movement by 50 ms. Due to correlations between velocity and acceleration, the neural activity was also related to acceleration. When applying a multiple regression analysis to neural activity and all movement parameters at the same time lag (as in Ashe & Georgopoulos, 1994), a significant relation with both velocity and acceleration emerged (permutation test $P < 0.01$; Materials and methods). Yet the apparent relation with acceleration resulted from inherent correlations between parameters and was not a property of the simulated neural activity.

Using the same artificial neural activity, we estimated the fraction of variance in the sample-to-sample firing rate profiles that is associated with end-point position, velocity, and/or acceleration (R^2), while taking into account temporal correlations between parameters (Materials and methods). For the data in this example, the highest R^2s were observed at a constant time lag relative to velocity, regardless of the time lag to position and/or acceleration (Fig. 2A). When teasing apart the contribution of different parameters to the movement-related variance, stripes on two faces of the velocity contribution cube are evident, making it apparent that velocity is dominant (Fig. 2B). Residual relations among movement parameters are expressed as patches in the position and acceleration cubes. This is possible as relations between parameters are not necessarily linear as assumed in the analysis (for instance, acceleration magnitude is not the time derivative of speed). There are no stripes on the faces of the position and acceleration cubes. Moreover, a dominant contribution to firing rate variance is evident as a plane of high values slicing through the velocity contribution cube at a fixed orientation (Fig. 2C). The plane indicates that the linear correlation between neural activity and velocity is at a constant lag regardless of the lags with other

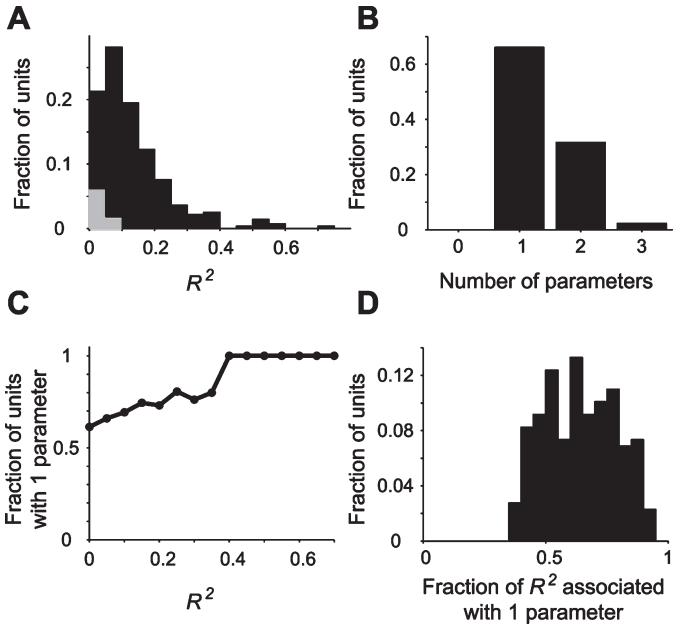

FIG. 4. Number of movement parameters correlated with neural activity. (A) Distribution of R^2 values. For each unit, the maximal R^2 over all combinations of time lags was noted. Units for which the value did not rank first in a permutation test (Materials and methods) are shown in grey. Histogram contains 277 units; bin width is 0.05. (B) Number of parameters related to a single motor cortical unit. Two-thirds of the movement-related units are related to a single parameter (66%, 144/218, all units with $R^2 > 0.05$). (C) Relation between R^2 and the single-unit tendency to be related to one dominant parameter. The fraction of units related to a single parameter depends on the R^2 threshold used. (D) Distribution of fractions of R^2 associated with a single parameter. For each unit, the parameter contributing the largest fraction of movement-related variance at the combination of time lags with the maximal R^2 was noted. Median contribution is 0.63, and 80% of the cases were above 0.5. Histogram contains 218 units and bin width is 0.05.

parameters. At this lag, the values in the velocity contribution cube are much higher than in the other cubes; in fact, all values were higher than 50% of the peak R^2. A full analysis of all slices through the cubes indicated that the putative neuron is related to velocity, but not to position or acceleration, at a constant time lag of 50 ms relative to movement. This is precisely what was simulated.

Arm-related motor-cortical units tend to be related to a single dominant parameter

Analysing the activity of real neurons in the manner detailed in Fig. 2 indicated that units were related to position, velocity, acceleration, as well as to multiple parameters (Fig. 3 shows some examples). In the first three examples, the highest contribution to the movement-related firing rate variance came from a set of time lags in a single plane cutting through one cube (Fig. 3A–C). While most of these neurons also showed some patchy relations to other parameters, this pattern was consistent with the pattern found in neural activity simulated based on a single parameter (e.g. Fig. 2B, top and bottom cubes). In contrast, some units were clearly related to more than one parameter (Fig. 3D) with a pattern identical to that found in neural activity simulated based on multiple parameters (see Materials and methods). At time lags common to two parameters, the movement-related variance is shared between them, so values at the intersection are lower. In sum, the examples are consistent with neural activity related to the movement parameter(s) at a constant time lag(s).

We applied the analysis to the activity of 277 well-isolated arm-related units recorded from the motor cortices of two monkeys (scribbling, 105 units; tracing, 172 units; see Materials and methods). Units were recorded during 115/157 scribbling/tracing trials (medians; 95% ranges 63–290/54–296) for a total duration of 4.4/7.4 min (medians; 95% ranges 2.6–10.4/2.8–14 min). Initially, analyses were carried out on units recorded during each of the tasks separately. Because results were consistent between the two tasks data were subsequently combined and are reported for the two tasks together. The vast majority of units were movement-related (255/277 units, 92%; permutation test $P < 0.01$), with a median maximal R^2 value of 0.10 (Fig. 4A). Of the 255 movement-related units, 218 had $R^2 > 0.05$ and were considered for further analyses, yielding a database of 218 units with a median R^2 value of 0.12.

The above R^2 values may seem low. However, this is not the case. For illustration, consider artificial firing rates generated on the basis of a model of tuning to velocity direction as in the previous section, employing movement data from centre-out experiments (five trials per direction). Averaging firing rates across movement time and all trials from the same direction yields R^2s that equal 0.93 (median; 95% range 0.75–0.99). However, the R^2s estimated for exactly the same data but on a sample-to-sample and trial-to-trial basis were much lower, with a median of 0.17 (95% range 0.09–0.26). Moreover, firing rates generated on the basis of the same model and continuous tracing movements of identical total duration yielded only slightly lower R^2s (median 0.16; 95% range 0.08–0.25; see also Fig. 2). To test whether low R^2 values in the real data result from the analysis technique, we made two additional tests. First, we applied an analysis that does not consider temporal correlations between parameters (Ashe & Georgopoulos, 1994) to the original sample of real units and continuous movements; the R^2s obtained were even lower (median, 0.09). Second, to determine whether the linearity assumption restricts the R^2 values in these data, we repeated the analysis using a nonlinear nonparametric technique (two-fold cross-validated support vector regression with a radial basis function kernel; Smola & Scholkopf, 2004). The median R^2 values obtained were 0.13, only slightly higher than for the linear model (mean improvement over cross-validated linear R^2 values, 5%; Mann–Whitney U-test $P = 0.7$). In short, the low R^2s did not result from task or computational specifics, but rather related the discharge variability of each firing rate profile to a highly variable set of movement parameters. Moreover, the R^2s were consistent with time-varying Poisson spike trains tuned to movement kinematics.

We classified the sample of units according to the number of parameters each unit was related to; for all movement-related units, there was at least one cube with a plane of high contribution (Fig. 4B). The majority of units (144/218, 66%) yielded a single plane of high contribution, indicating a fixed relation with a single dominant movement parameter. We tested whether the number of units related to a single parameter matched the number expected based on the hypothesis that parameters are distributed at random among the units. There was a clear and significant excess of units related to exactly one parameter (binomial test $P << 0.001$; Materials and methods). Thus, a single motor cortical neuron tended to be related to a single dominant movement parameter.

Next we examined the robustness and generality of the above result. As the overall correlation with movement kinematics improved, the probability of units to be related to a single parameter increased. For quantification, we varied the R^2 used as a threshold for inclusion of units in the analysis (Fig. 4C); in the extreme case, all measured units with R^2s above 0.4 were related to a single parameter.

Identifying a relation to a single dominant parameter involves the detection of planes and depends on the criterion used for defining

dominance. To verify that the tendency to covary with a single parameter does not depend on the existence of high contribution planes, we focused on the time lags with the highest R^2 values. For each unit, we noted the fraction of movement-related variance contributed by the most dominant parameter; for 80% of the units, a single parameter contributed over half of the movement-related variance (Fig. 4D). The median contribution of the most dominant parameter was 63% of the maximal R^2, well above 50%, the threshold used for defining a relation to a single dominant parameter.

The movement model used above included a set of behavioural (movement) parameters, but it is possible that the activity of a unit also depends on its past activity. We thus considered an extended auto-regressive model that accounted for potential serial correlations in firing (Materials and methods). The discharge of 259/277 units (94%) varied with this model (permutation test $P < 0.01$), with a median R^2 value of 0.15. Thus, the extended model yielded higher R^2s than the original model (medians of 218 units 0.18 vs. 0.12; *U*-test $P << 0.001$), with a median contribution of 26% from the auto-regressive term. Yet more than half of the units were still related to a single predominant parameter (118/218 units, 54%). Moreover, for each unit the pattern of contributions of movement parameters was almost identical to that obtained for the original model (median correlation-coefficient 0.98; 95% range 0.33–0.99).

Finally, to test whether the predominance of single parameters depended on brain region, we divided the sample of movement-related units into two groups, corresponding to units recorded in M1 (90 units) and PMd (128 units). In both regions there was an excess of units related to a single parameter (63/90, 70%, and 81/128, 63%; binomial tests $P < 0.01$ for each region). The fractions of units related to a single dominant parameter were similar for the two regions (χ^2 test of independence $\chi^2 = 1.06$, $P = 0.3$). Thus, the tendency of single units to be related to a single movement parameter seemed to be a consistent property that did not depend on arbitrary definitions, computational specifics, or past firing activity, and was obtained for both tested brain regions.

The most commonly represented kinematic parameter is velocity

As approximately one-third of the units were related to more than one parameter (Fig. 4B), the number of significant unit-parameter relations (297, henceforth referred to as all 'represented' parameters) was larger than the number of units (218). For the analysis of parameter identity, we first focused on units related to a single parameter (144 units; Table 1, first row). Most units were related to velocity (115/144, 80%). The fraction of units related to velocity was higher than expected assuming equal representation of the three tested parameters (χ^2 goodness-of-fit test $n = 144$, $\chi^2 = 140$, $P << 0.001$). Similar results were obtained when basing the decision on the parameter with the maximal contribution at any combination of time lags and when all represented parameters were considered (Table 1, second and third rows, respectively). Moreover, there were no differences in the parameter distributions between M1 and PMd (63 and 81 units, χ^2 test of independence 3×2 table, $\chi^2 = 1.86$, $P = 0.39$). In both regions velocity was the most common parameter as 76% M1 and 83% PMd units were related to velocity.

TABLE 1. Distributions of kinematic parameters correlated with neural activity

	Position	Velocity	Acceleration	Total
Units related to one parameter	13 (9%)	115 (80%)	16 (11%)	144 units
Highest contribution	22 (10%)	154 (71%)	42 (19%)	218 units
All represented parameters	41 (14%)	187 (63%)	69 (23%)	297 parameters

To determine whether encoding strength differs between units related to different parameters, we estimated median R^2s for units related to each parameter. The movement-related portions of firing rate variance of units related to position, velocity, and acceleration were 0.14, 0.13, and 0.12 (medians of 13, 115, and 16 units, respectively) and were not significantly different from one another (Kruskal–Wallis nonparametric ANOVA $P = 0.73$). Similar results were obtained when considering all represented parameters and when considering maximal contribution values over different parameters instead of R^2s. Thus, despite the ubiquity of velocity relations, subsets of units related to other parameters modulated their firing rate with movement to a similar degree as the velocity-related units.

We also considered the amplitude and direction of the velocity and the acceleration vectors as separate parameters, yielding a total of five movement parameters (Table 2). Note that the separation is not complete because direction is still scaled by amplitude (Materials and methods; Moran & Schwartz, 1999). Of the units related to velocity, more than 90% were related to the direction of the velocity vector (Table 2, first row). R^2 values were similar for all five parameters (Table 2, second row; nonparametric ANOVA $P = 0.17$). In sum, even when temporal correlations between movement parameters were explicitly considered, most motor cortical neurons were related to velocity.

Time lags between neural activity and movement are dispersed and depend loosely on anatomy

For units related to a single dominant movement parameter as well as for all represented parameters, the average time lag was significantly greater than zero, indicating a tendency of firing rates to precede motion (one-tailed *t*-tests $P << 0.001$ with $n = 144$ and 297 parameters, respectively; mean time lag and SD 44 ± 94 and 56 ± 106 ms; lags were normally distributed for both samples, Bera–Jarque tests $P = 0.074$ and 0.28). Notably, the dispersion of time lags was large

TABLE 2. Distributions of parameters correlated with neural activity, five parameters considered

	Position	Velocity direction	Velocity amplitude	Acceleration direction	Acceleration amplitude	Total
Units related to one parameter	17 (12%)	104 (74%)	4 (3%)	12 (9%)	3 (2%)	140 units *
Median $R^{2\dagger}$	0.14	0.15	0.08	0.12	0.11	0.13
Highest contribution	21 (10%)	151 (69%)	11 (5%)	26 (12%)	9 (4%)	218 units
All represented parameters	51 (17%)	168 (55%)	24 (8%)	49 (16%)	13 (4%)	305 parameters

*When describing motion by five parameters, a few units that were categorized in Table 1 as related to one parameter appeared as related to two (amplitude and direction). One-hundred and twenty-nine units were categorized as related to a single parameter in both descriptions. †Of units related to one parameter.

(Fig. 5A). In both samples, 28% of the parameters had negative delays, suggesting a relationship to feedback of the executed motion. For the 74 units related to more than one parameter, time lags for different parameters typically differed, the median absolute time lag difference being 120 ms (84 parameter pairs). There were no consistent differences between time lags of different parameters (Fig. 5B).

We examined the relationship between time lags and the anatomical location of the recorded units. While the overall median time lag was 60 ms (297 parameters), lags were shorter for units recorded closer to the central sulcus (nonparametric ANOVA $P < 0.01$; Fig. 5C). The median time lag in M1 was 40 ms (120 parameters) while in PMd it was 80 ms (177 parameters). The fraction of parameters with a negative time lag was 33% and 20% in M1 and PMd, respectively. Similar results were obtained for units related to a single parameter. Thus, although in all other tested aspects M1 and PMd were similar, neural activity in PMd tended to be related to movement before M1 activity. However, in both regions a substantial portion of activity came either together with or after motion.

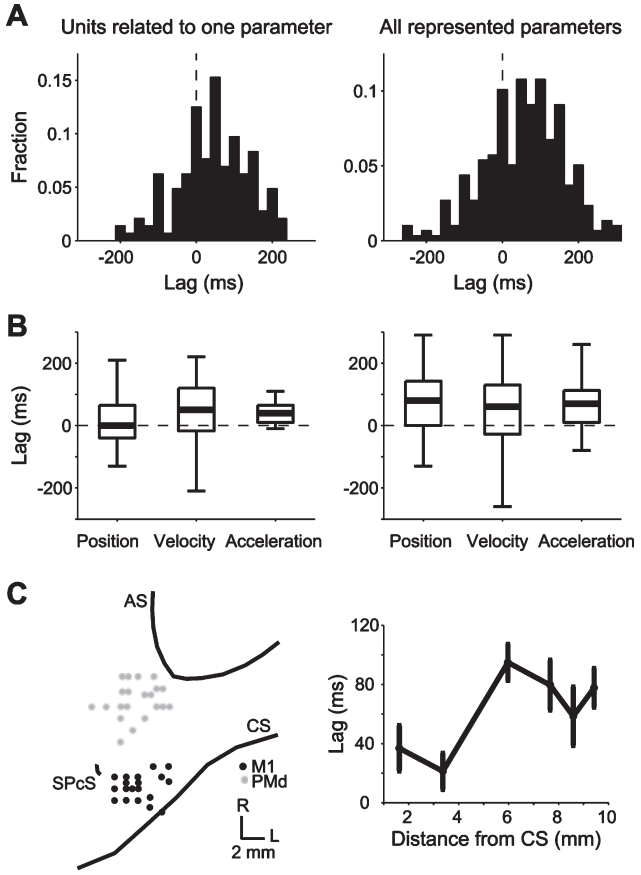

FIG. 5. Time lags between neural activity and movement. (A) Distributions of time lags. The left panel shows time lags of units related to a single dominant parameter (144 units), and the right panel shows the distribution of time lags of all represented parameters (297 parameters). Bin width is 25 ms in both histograms. There is a tendency for time lags to be positive, corresponding to neural activity coming before movement. (B) Time lags for separate parameters. The left panel shows time lags for units with a single dominant parameter, and the right panel shows time lags for all parameters. Sample sizes are detailed in Table 1, first and third rows. In each panel, thick lines show medians, thin lines show upper and lower quartiles, and whiskers extend to cover all samples within 1.5 times the interquartile range. There are no consistent differences between time lags of different parameters. (C) Dependence of time lags on cortical region. (Left panel) Distribution of recording sites on the cortical surface. Anatomical reconstruction was performed separately for each monkey (see Materials and methods); as one hemisphere was left (monkey U) it was reflected relative to the midline and repositioned to maximize the overlap between the anatomical landmarks. Here, a site refers to guide tube position and included up to eight microelectrodes (see Materials and methods). Seven well-isolated units were recorded from each site (median; 95% range, 2–12). AS, arcuate sulcus; CS, central sulcus; L, lateral; R, rostral; SPcS, superior precentral sulcus. (Right panel) Parameters were divided into six equal-sized bins according to the distance of the corresponding recording site from the CS (49–50 parameters/bin). Time lags were then averaged for each bin; error bars show SEM. Although activation overlaps, neural activity in PMd tends to precede M1 activity.

Forearm muscles tend to be related to a single kinematic movement parameter

We recorded the activity of several shoulder and elbow muscles on separate sessions from the neuronal recordings. During the tracing task, different muscles were related to different parameters. For instance, the deltoid was related mainly to position but also to velocity, while other muscles were related mainly to velocity or acceleration (Fig. 6A). Overall, a sizable fraction of muscle activity variance was associated with the linear kinematic model, as muscles had R^2s of 0.35 (median of 17 muscle recordings), significantly higher than the median R^2 of single-units (U-test $P << 0.001$; Fig. 6B).

A more detailed inspection showed that muscles, like motor cortical units, tended to be related to a single dominant parameter (Fig. 6C), most often velocity (Fig. 6D). The only tested muscle related to position was the deltoid, and – perhaps surprisingly – the only muscle related predominantly to acceleration was the biceps. The median time lag for muscles was 120 ms, longer than the median time lag for units, which was 60 ms (U-test $P = 0.012$; Fig. 6E). In contrast to units, no muscle had a negative time lag.

Discussion

Using tasks that broadly sampled kinematic movement parameters in a planar workspace, we found that almost all tested motor cortical neurons were movement-related, and that most neurons were related to a single dominant parameter. The most common parameter was velocity. Forearm muscles displayed similar properties, but while muscle activity preceded movement, the time lags of neural activity were widely distributed in both M1 and PMd.

Neural activity related to single or multiple kinematic parameters

Previous studies of straight reaching movements showed that single neuron activity may be related to multiple parameters, either at the same time (Ashe & Georgopolous, 1994; Messier & Kalaska, 2000; Paninski *et al*., 2004) or at different times (Fu *et al*., 1995; Johnson *et al*., 1999; Gomez *et al*., 2000). In the current study multiple movement parameters were explicitly considered and yet single neuron activity was typically related to a single predominant parameter. There are two methodological differences between the previous and the current work that may account for this difference.

First, movement tasks differed. In prior work multiple repetitions of stereotypical movements were obtained, and in some studies, subjects were required to focus on different parameters at different points in time (Fu *et al*., 1995; Johnson *et al*., 1999; Gomez *et al*., 2000). In contrast, the current tasks yielded highly variable motion; hence movement parameters and combinations of parameters were well-sampled, providing the possibility to differentiate one parameter from another. The fact that results were consistent across two tasks further increases their reliability. While the two tasks placed different

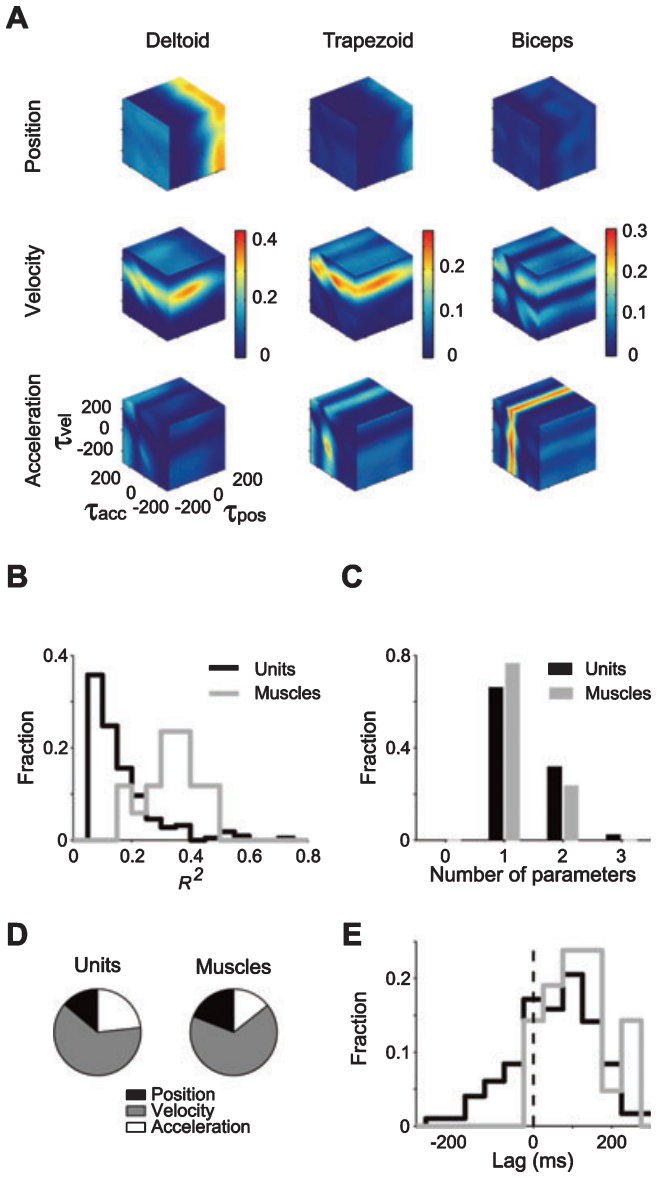

FIG. 6. Correlations between muscle activity and kinematic parameters. (A, left) Deltoid activity is related to position and velocity, with a maximal R^2 of 0.45. Time lag is 230 ms for position and 90 ms for velocity. (Center) Trapezoid activity is mainly related to velocity, with a time lag of 160 ms; R^2 is 0.27. (Right) Biceps activity is mainly related to acceleration with a time lag of 50 ms and R^2 of 0.32. Conventions are the same as in Fig. 2B. (B) Distributions of R^2 values for motor cortical units (black) and forearm muscles (grey). Histograms contain 218 units and 17 muscle recordings; bin width is 0.05. R^2 values for muscles are higher. (C) Number of parameters each unit (black) or muscle (grey) is related to. Sample sizes are the same as in (B) and conventions are the same as in Fig. 4B. Both units and muscles tend to be related to a single dominant parameter. (D) Distributions of kinematic parameters correlated with unit (left) and muscle (right) activity. There are 297 parameters for units and 21 for muscles. For both units and muscles, the most common parameter is velocity. (E) Distributions of time lags for parameters correlated with unit (black) and muscle (grey) activity. Sample sizes are the same as in (D) and bin width is 50 ms. In contrast to the widely distributed time lags for units, time lags for muscles were all positive, indicating a tendency for muscle activity to come before movement.

requirements on the monkeys and clearly differed from a motor control perspective, both provided broad sampling of motion, reduced correlations at zero-lag, and nearly identical results.

Second, the method of analysis differed. While previous studies ignored temporal correlations between parameters, the current analysis extended previous applications of multiple linear regression analysis by explicitly considering delayed interdependencies, exploiting the fact that parameters were not perfectly correlated at any time lag (in which case there would have been no way to separate their contributions). Based on analyses that considered the temporal sequence in a task but ignored temporal correlations between position and velocity, parameters, which are clearly not independent, it has been suggested that a temporal parcellation encoding scheme is useful for accommodating neural activity with varying task demands (Johnson *et al.*, 2001). Because of the differences in tasks and analyses, the current findings cannot be interpreted as being at odds with encoding by temporal parcellation. Rather, they emphasize the relation of a single neuron to a single parameter during continuous movements.

Neural activity related predominantly to velocity

The most common dominant parameter was hand velocity. This result is consistent with the large body of literature reporting that velocity direction, with or without speed scaling, is a prominent parameter encoded by motor cortex neurons during straight reaching (Georgopoulos *et al.*, 1982, 1986) and curved movements (Schwartz, 1992; Moran & Schwartz, 1999; Paninski *et al.*, 2004). The current results extend these findings by using new behavioural paradigms in which movement parameters were wholly (scribbling) or partially (tracing) determined by monkeys and by explicitly considering additional kinematic parameters, position and acceleration.

For position, we used a cosine model as it captures the idea of a preferred position with gradual decline of firing rate around it. Others have used a model of monotonous planar sensitivity (Kettner *et al.*, 1988; Paninski *et al.*, 2004), effectively measuring the 'direction' of the position and requiring an arbitrary decision about the position of an origin (e.g. 0, 0) from which direction is measured. We compared our cosine model with the planar and Gaussian models (Aflalo & Graziano, 2006); for the current data, Gaussian was somewhat better than cosine and both were better then a planar model. When the planar model was used, R^2s were slightly lower (median, 0.11) but the main results were unaltered (64% of the units were related to a single parameter, most often velocity). For velocity and acceleration, we employed a model in which direction was scaled by amplitude (Moran & Schwartz, 1999), capturing the idea that neural activity is unlikely to be modulated by direction in the lack of movement. Again, similar results were obtained when directions were considered without amplitude scaling.

Notably, the neurons related to position or acceleration yielded R^2s similar to those related to velocity. Thus, the current results suggest that even when temporal correlations between kinematic parameters are considered, velocity relations are more commonly represented, yet not necessarily stronger, in the activity of motor cortical neurons.

While it is highly unlikely that the relation to velocity is an epiphenomenon of a relation to another kinematic parameter in the set of tested parameters, the possibility remains that other parameters, not measured or included in the current study, are responsible for the observed relations. Past firing made an important contribution to firing variability, but did not alter the relative contributions of the movement parameters included. For the tracing task, one potentially important parameter is the visually instructed path. As the actual paths were almost identical to the instructed paths, the two were not dissociated. For both tasks, it is possible that if movement was measured in other frames of reference, the activity of a single neuron would be related to

multiple highly interdependent parameters, such as the activity of several muscles.

Muscle activity and coordinate frames

Akin to the neural activity, muscle activity was predominantly related to the velocity measured in extrinsic coordinates. This result is consistent with the theoretical prediction that when movement is measured in a small workspace (in the current study, approximately 100 cm^2), neural activity purely related to muscle activity may appear to be related to velocity (Todorov, 2000). Moreover, in a small workspace parameters from different coordinate frames are highly correlated (Reina *et al*., 2001) and hence difficult to separate. Thus, our results cannot be taken as evidence that motor cortex encodes movement in any specific (extrinsic or intrinsic, kinematic or kinetic) frame of coordinates. While several studies have studied the coordinate frame in which motor cortical neurons represent movement (Scott *et al*., 2001), the coordinate frame might differ for different neurons (Kakei *et al*., 1999) and perhaps change with task demands (Fetz, 1992).

While considerably more diverse than used in most relevant previous studies, the current behavioural dataset is less diverse than the full range of natural movement. Recent technological advances provide means to monitor behaviour under more natural circumstances (e.g. Aflalo & Graziano, 2006; Jackson *et al*., 2006). Thus, future studies that will explicitly consider temporal correlations between movement parameters (kinematic parameters and muscle activity) during natural movements and/or under loading conditions may help clarify the coordinate frame issue.

Movement signal and neural noise

In most cases, the fraction of firing rate variance related to the tested parameters was small, on the order of 0.1–0.2 for linear and nonlinear models alike. These values may seem low compared to studies reporting R^2 values above 0.7 (e.g. Georgopoulos *et al*., 1982), but such a comparison is invalid as these studies typically minimize variability in neural activity by minimizing variability in all except the tested parameter and report R^2s for time- and trial-averaged data.

A more appropriate comparison is with studies that conduct time-course analyses of single trials (Ashe & Georgopoulos, 1994) or rich sampling of movement parameters (Paninski *et al*., 2004; Aflalo & Graziano, 2006). Such studies typically report low R^2s, which may indicate relations with other variables not considered in the analysis. However, in the current data, muscles yielded higher R^2s than neurons, suggesting that the low R^2s may alternatively result from inherent neuronal noise. Consistent with this interpretation, we showed that low R^2s are obtained when neural activity is modelled as a movement-dependent time-varying Poisson process (but see DeWeese *et al*., 2003).

Dispersion of time lags

Previous studies have emphasized that activity of motor cortical neurons precedes movement, peaking approximately 100 ms prior to movement. We found the same general tendency, but the average time lags were shorter, in the order of 50 ms. This may be related to the fact that movement speed in the tasks used here was higher than reported in other studies (Johnson *et al*., 1999; Reina *et al*., 2001; Paninski *et al*., 2004). Another cause may be feedback during task performance. While feedback might play a negligible role during stereotypical motion, it could be important for executing complex, constantly changing movements as used here (Wolpert & Ghahramani, 2000).

While muscles exhibited strictly positive time lags, approximately one-quarter of the neuronal time lags were negative, corresponding to the bulk of neural activity coming after movement. Although not always emphasized, dispersion was also evident in other studies (Thach, 1978; Ashe & Georgopoulos, 1994; Schwartz *et al*., 2004). Long negative lags can come from muscles and joints. However, proprioceptive feedback is delayed tens of milliseconds before reaching the cortex. Thus, small negative lags may represent an internal (efference) copy of a motor command. Moreover, as there is a delay between cortical activity and a resulting measurable movement, neurons with a small positive time lag are certainly not activating movement. In short, neurons with lags around zero participate in processes other than movement planning, activation, or sensory feedback, for example, in internal models (Kawato, 1999) useful for predicting movement errors or generating correcting commands.

Neural activity in the PMd tended to precede activity in M1. This confirms the results of previous studies (Kalaska & Crammond, 1992; Moran & Schwartz, 1999) and is consistent with the more prominent preparatory activity in the PMd than in M1 and the proposed role of the premotor cortex in movement planning (Weinrich & Wise, 1982). Time lags were highly variable in both motor regions, consistent with motor cortex involvement in a wide range of movement-related internal processes such as movement planning and execution (Alexander & Crutcher, 1990).

Possible functional implications

What is the computational advantage of a dominant relation to a single parameter, when behaviour is obviously composed of a rich set of parameters? If spikes from a given neuron were ‘stamped’ as being related to a given parameter by virtue of the source neuron, then there would be no need for other neural networks such as the spinal cord to de-multiplex the neural signal, greatly simplifying communication between neural structures. The observation that single muscles also tend to be related to a single kinematic parameter supports this possibility.

However, not all motor cortical neurons are ‘output’ neurons. Rather, a considerable part of M1 and PMd activity is likely to be related to internal processes and computations that precede, proceed, or occur concurrently with movement and might depend on the behavioural context. The widely distributed time lags are consistent with this possibility and may reflect a range of movement-related internal processes. In this regard, our results suggest that distinct neurons partake in internal computations related to different movement parameters.

Acknowledgements

We thank Hagai Bergman for critical reading of a previous version of the manuscript, Gadi Goelman for MRI scans, Zoltan Nadasdy for help in experiments, Moshe Nakar for setup construction, Varda Sharkansky for technical assistance, and Eilon Vaadia for helpful suggestions. This study was supported in part by a Center of Excellence grant (1564/04) administered by the Israel Science Foundation and the Deutsch-Israelische Projectkooperation.

Abbreviations

M1, primary motor cortex; PMd, dorsal premotor cortex.

References

Aflalo, T.N. & Graziano, M.S. (2006) Partial tuning of motor cortex neurons to final posture in a free-moving paradigm. *Proc. Natl Acad. Sci. USA*, **103**, 2909–2914.

Alexander, G.E. & Crutcher, M.D. (1990) Neural representations of the target (goal) of visually guided arm movements in three motor areas of the monkey. *J. Neurophysiol.*, **64**, 164–178.

Ashe, J. & Georgopoulos, A.P. (1994) Movement parameters and neural activity in motor cortex and area 5. *Cereb. Cortex*, **4**, 590–600.

Caminiti, R., Johnson, P.B. & Urbano, A. (1990) Making arm movements within different parts of space: dynamic aspects in the primate motor cortex. *J. Neurosci.*, **10**, 2039–2058.

Carpenter, A.F., Georgopoulos, A.P. & Pellizzer, G. (1999) Motor cortical encoding of serial order in a context-recall task. *Science*, **283**, 1752–1757.

Crutcher, M.D. & Alexander, G.E. (1990) Movement-related neuronal activity selectively coding either direction or muscle pattern in three motor areas of the monkey. *J. Neurophysiol.*, **64**, 151–163.

DeWeese, M.R., Wehr, M. & Zador, A.M. (2003) Binary spiking in auditory cortex. *J. Neurosci.*, **23**, 7940–7949.

Draper, N.R. & Smith, H. (1981) *Applied Regression Analysis*. John Wiley and Sons, New York.

Evarts, E.V. (1968) Relation of pyramidal tract activity to force exerted during voluntary movement. *J. Neurophysiol.*, **31**, 14–27.

Fetz, E.E. (1992) Are movement parameters recognizably coded in activity of single neurons? *Behav. Brain Sci.*, **15**, 679–690.

Fetz, E.E. & Cheney, P.D. (1980) Postspike facilitation of forelimb muscle activity by primate corticomotoneuronal cells. *J. Neurophysiol.*, **44**, 751–772.

Flament, D. & Hore, J. (1988) Relations of motor cortex neural discharge to kinematics of passive and active elbow movements in the monkey. *J. Neurophysiol.*, **60**, 1268–1284.

Fu, Q.G., Flament, D., Coltz, J.D. & Ebner, T.J. (1995) Temporal encoding of movement kinematics in the discharge of primate primary motor and premotor neurons. *J. Neurophysiol.*, **73**, 836–854.

Georgopoulos, A.P., Ashe, J., Smyrnis, N. & Taira, M. (1992) The motor cortex and the coding of force. *Science*, **256**, 1692–1695.

Georgopoulos, A.P., Kalaska, J.F., Caminiti, R. & Massey, J.T. (1982) On the relations between the direction of two-dimensional arm movements and cell discharge in primate motor cortex. *J. Neurosci.*, **2**, 1527–1537.

Georgopoulos, A.P., Schwartz, A.B. & Kettner, R.E. (1986) Neuronal population coding of movement direction. *Science*, **233**, 1416–1419.

Gomez, J.E., Fu, Q., Flament, D. & Ebner, T.J. (2000) Representation of accuracy in the dorsal premotor cortex. *Eur. J. Neurosci.*, **12**, 3748–3760.

Humphrey, D.R., Schmidt, E.M. & Thompson, W.D. (1970) Predicting measures of motor performance from multiple cortical spike trains. *Science*, **170**, 758–762.

Jackson, A., Mavoori, J. & Fetz, E.E. (2006) Long-term motor cortex plasticity induced by an electronic neural implant. *Nature*, **444**, 56–60.

Johnson, M.T., Coltz, J.D. & Ebner, T.J. (1999) Encoding of target direction and speed during visual instruction and arm tracking in dorsal premotor and primary motor cortical neurons. *Eur. J. Neurosci.*, **11**, 4433–4445.

Johnson, M.T., Mason, C.R. & Ebner, T.J. (2001) Central processes for the multiparametric control of arm movements in primates. *Curr. Opin. Neurobiol.*, **11**, 684–688.

Kakei, S., Hoffman, D.S. & Strick, P.L. (1999) Muscle and movement representations in the primary motor cortex. *Science*, **285**, 2136–2139.

Kalaska, J.F. & Crammond, D.J. (1992) Cerebral cortical mechanisms of reaching movements. *Science*, **255**, 1517–1523.

Kawato, M. (1999) Internal models for motor control and trajectory planning. *Curr. Opin. Neurobiol.*, **9**, 718–727.

Kettner, R.E., Schwartz, A.B. & Georgopoulos, A.P. (1988) Primate motor cortex and free arm movements to visual targets in three-dimensional space. III. Positional gradients and population coding of movement direction from various movement origins. *J. Neurosci.*, **8**, 2938–2947.

Kurata, K. (1993) Premotor cortex of monkeys: set- and movement-related activity reflecting amplitude and direction of wrist movements. *J. Neurophysiol.*, **69**, 187–200.

Messier, J. & Kalaska, J.F. (2000) Covariation of primate dorsal premotor cell activity with direction and amplitude during a memorized-delay reaching task. *J. Neurophysiol.*, **84**, 152–165.

Moran, D.W. & Schwartz, A.B. (1999) Motor cortical representation of speed and direction during reaching. *J. Neurophysiol.*, **82**, 2676–2692.

Mussa-Ivaldi, F.A. (1988) Do neurons in the motor cortex encode movement direction? An alternative hypothesis. *Neurosci. Lett.*, **91**, 106–111.

Paninski, L., Fellows, M.R., Hatsopoulos, N.G. & Donoghue, J.P. (2004) Spatiotemporal tuning of motor cortical neurons for hand position and velocity. *J. Neurophysiol.*, **91**, 515–532.

Park, M.C., Belhaj-Saif, A. & Cheney, P.D. (2004) Properties of primary motor cortex output to forelimb muscles in rhesus macaques. *J. Neurophysiol.*, **92**, 2968–2984.

Reina, G.A., Moran, D.W. & Schwartz, A.B. (2001) On the relationship between joint angular velocity and motor cortical discharge during reaching. *J. Neurophysiol.*, **85**, 2576–2589.

Riehle, A. & Requin, J. (1995) Neuronal correlates of the specification of movement direction and force in four cortical areas of the monkey. *Behav. Brain Res.*, **70**, 1–13.

Scherrer, B. (1984) *Biostatistque*. Gaetan Morin, Boucherville.

Schwartz, A.B. (1992) Motor cortical activity during drawing movements: single-unit activity during sinusoid tracing. *J. Neurophysiol.*, **68**, 528–541.

Schwartz, A.B. (1994) Direct cortical representation of drawing. *Science*, **265**, 540–542.

Schwartz, A.B., Kettner, R.E. & Georgopoulos, A.P. (1988) Primate motor cortex and free arm movements to visual targets in three-dimensional space. I. Relations between single cell discharge and direction of movement. *J. Neurosci.*, **8**, 2913–2927.

Schwartz, A.B., Moran, D.W. & Reina, G.A. (2004) Differential representation of perception and action in the frontal cortex. *Science*, **303**, 380–383.

Scott, S.H., Gribble, P.L., Graham, K.M. & Cabel, D.W. (2001) Dissociation between hand motion and population vectors from neural activity in motor cortex. *Nature*, **413**, 161–165.

Scott, S.H. & Kalaska, J.F. (1997) Reaching movements with similar hand paths but different arm orientations. I. Activity of individual cells in motor cortex. *J. Neurophysiol.*, **77**, 826–852.

Sergio, L.E., Hamel-Paquet, C. & Kalaska, J.F. (2005) Motor cortex neural correlates of output kinematics and kinetics during isometric-force and arm-reaching tasks. *J. Neurophysiol.*, **94**, 2353–2378.

Smola, A. & Scholkopf, B. (2004) A tutorial on support vector regression. *Stat. Comput.*, **14**, 199–222.

Stark, E., Drori, R. & Abeles, M. (2006) Partial cross-correlation analysis resolves ambiguity in the encoding of multiple movement features. *J. Neurophysiol.*, **95**, 1966–1975.

Thach, W.T. (1978) Correlation of neural discharge with pattern and force of muscular activity, joint position, and direction of intended next movement in motor cortex and cerebellum. *J. Neurophysiol.*, **41**, 654–676.

Todorov, E. (2000) Direct cortical control of muscle activation in voluntary arm movements: a model. *Nature Neurosci.*, **3**, 391–398.

Weinrich, M. & Wise, S.P. (1982) The premotor cortex of the monkey. *J. Neurosci.*, **2**, 1329–1345.

Wolpert, D.M. & Ghahramani, Z. (2000) Computational principles of movement neuroscience. *Nature Neurosci.*, **3**, 1212–1217.